ИНСТИТУТ ЯДЕРНОЙ ФИЗИКИ
им. Г.И. Будкера СО РАН

А.С. Александров, А.И. Горбовский, В.В. Мишагин,
А.В. Ситников, К.К. Шрайнер, Г.Ф. Абдрашитов,
Е.Д. Бендер, А.А. Иванов, И.А. Котельников,
А.А. Подыминогин, Ю.С. Попов, Ю.А. Цидулко

РАЗРАБОТКА ОСНОВНЫХ КОНСТРУКТИВНЫХ ХАРАКТЕРИСТИК МАГНИТНОЙ СИСТЕМЫ ВОДОРОДНОГО ПРОТОТИПА ИСТОЧНИКА НЕЙТРОНОВ

ИЯФ 94-7

НОВОСИБИРСК

Elaboration of the principal design characteristics of the magnetic system for the Hydrogen Prototype of the Neutron Source.

A.S.Alexandrov, A.I.Gorbovsky, V.V.Mishagin, A.V.Sitnikov, K.K.Schreiner, G.F.Abdrashitov, E.D.Bender, A.A.Ivanov, I.A.Kotel'nikov, A.A.Pod'minogin, Yu.S.Popov, and Yu.A.Tsidulko

Budker Institute of Nuclear Physics, 630090, Novosibirsk, Russia

Abstract.

The paper reviews designs of magnets and vacuum system of the Hydrogen Prototype of the Neutron Source. An idea of this neutron source is based on the use of neutral-beam-driven plasma in an axisymmetric magnetic mirror to generate high flux D-T neutrons. Preliminary evaluations have shown that such a source has several potential advantages when is used for fusion material and component tests. The Hydrogen Prototype is essentially full scale model of the source but operated with a hydrogen plasma. Plasma physics tests can be then properly done at the device without the hampering neutron irradiation.

INTRODUCTION

The present research has been done to develop main design solutions for magnetic coils of the Hydrogen Prototype of the Neutron Source (acronym HPNS) based on a gas-dynamic trap concept. It also includes a conceptual design of the vacuum system of the device.

The paper is organized as follows:

Section 1 is devoted to the general description of the central cell coil set and presents calculated parameters of the magnetic field. Here the characteristics of the chosen power supply for the magnets are described too. A technology for manufacturing the coils in the INP machine shop is briefly discussed in this section. Section 2 gives the design of mirror magnets. These magnets produce on-axis magnetic field of about 20 Tesla and operate under extremely strong ponderomotive forces. Therefore their design has to be different

from that of the central cell coils. We considered a layout where the magnets are composed of outer and inner sections. The first one is powered in series with the central cell coils while the inner small radius insert is independently energized from a capacitor bank in 150 ms pulses. The heat released during the pulse is removed between shots by air cooling from the side walls of the inserts. Such a realization allows the mirror ratio to be variable in the range from 8 to 20. In Section 3 we give a description of the vacuum system of the Hydrogen Prototype. This subject has not been initially included into the scope of the work. Nevertheless after the design has been started, almost from the very beginning, we recognized that both systems cannot be designed separately. For example, which is probably the most simple one, periodical baking of the main vacuum chamber demands for the coils to be thermo- and mechanically insulated from the chamber. We also have decided to include into the present paper the structure of the first wall that is described in Section 4. The final section presents the design of the plasma dumps which are to be installed inside the end tanks.

The Hydrogen Prototype is intended to generate a plasma physics database at plasma parameters as close as possible to those expected in the GDT-based neutron source. This mission determined the approach to its design as an experimental facility with sufficiently high flexibility and pulse mode operation using power supplies available at the INP site. Initial data for the design of the HPNS magnetic system were formulated to meet both plasma physics requirements and technological constraints. Plasma-physical considerations involved the MHD-stability analysis, particle and energy balances and adiabaticity of the sloshing ion motion in the central cell. The number of ion Larmor radii on a plasma radius was required to be at least 2-3 in order to avoid density-gradient-driven instabilities. At energy of the HPNS's neutral beams of 40keV, this condition implies a minimum value of the magnetic field at the midplane of 0.4-0.6T for hydrogen ion of full energy. According to these considerations, the magnetic field strength at the center of the device was chosen to be 1T.

We have considered errors of the magnetic field that could be induced by misalignments of the coils and distortions of their shape. As a result, requirements to the coil production technology and the accuracy of its assembling procedure have been formulated. These errors, as being of a small value, can be treated analytically in dipole or/and quadrupole approximation. The dipole perturbation could be induced by an offset of a coil from the geometrical axis and/or rotation of the coil by a small angle around one of its diameter. Another cause of the perturbations is a finite transverse size of the conductor.

In this case a current has to have both azimuthal and radial components located at the transitions between different layers of turns. Magnetic fields generated by these transitions and local feeds contribute also to dipole disturbances. Quadrupole perturbations are induced by small deviations of coil shapes from ideal circular ones. Perturbations of both types can be provoked also by metallic parts located near the device that may have significant magnetic moments induced by stray magnetic fields of the device. In turn, errors of the magnetic field cause an offset of the plasma column from the geometrical axis and force it to be elliptical in cross section. These errors may also give rise to undesirable enhanced drifts of the sloshing ions and provoke the lost of adiabaticity of their motion. Coil design and assembly tolerances have been chosen to reduce the amplitude of dipole perturbations to less than 0.001 of the main on-axis magnetic field. Our estimations show that perturbations of such a small value can be neglected. Nevertheless a set of compensating coils will be also installed at the end tanks to reduce further the distortions of the plasma equilibrium. Recently we have studied on the GDT facility a plasma response to multipole magnetic perturbations that were externally applied in the expander region. These experiments have shown reasonable efficiency of the compensating system composed of two pairs of coils azimuthally shifted by 90 degrees. However, it can only reduce distortions of plasma equilibrium controlled by external fields averaged along the entire device. Nevertheless perturbations of the sloshing ion orbits still require to be compensated locally.

The main requirements for the magnetic system layout were the following:

1. The mirror ratio is to be varied from 8 to 20 at 1 Tesla constant magnetic field at the midplane. The distance between mirrors is 10m.
2. The main magnetic system is powered by 25kA current. Pulse duration is 2s in an equivalent dc-current with the flattop of 0.5s. Pulse repetition rate: one shot in every 20min.
3. Capabilities of the power supply available at the site limit the total power consumption of the coils to 40MW.
4. In the coil set-up one should take into account easy access to diagnostic and other ports in the main vacuum chamber.
5. The coils should be unified in size, production technology and use available copper conductors.

One of the parameters that substantially affect the magnetic coil design is the injection angle of the neutral beams. In order to maximize the sloshing ion density at the

turning points the angle should be as small as possible. On the other hand, it cannot be too small in order to avoid a decrease in the sloshing ion lifetime due to an increased scattering rate into the loss cone. Technically, it also turns out to be very difficult to obtain injection angles less than 30 degrees. In this case the gap between the coils, where the neutral beams are passing through, becomes inadmissibly large. As a compromise between the above mentioned physical and design limitations, the injection angle was taken to be 30 degrees. Figure 1 shows the general pattern of the device. As can be seen from this cut-away drawing, the device has four neutral beam injectors aimed at its center. Untrapped beams enter the dumps located opposite to the injectors where they are partially implanted into end plates or reflected as low energy neutrals. In order to prevent the scattered neutrals from coming back into the central cell, it was decided to evaporate titanium on the inner walls of the dumps.

The main parameters of the magnetic system are listed in Tables 1.1, 1.2. Indicated in parentheses are the values that correspond to the initial stage of the operation of the facility when only the existing transformer is used providing a half of the nominal electric power to the coils.

Central cell coils

Table 1.1

Magnetic field at midplane, T	1(0.7)
Mirror ratio	8-20
Mirror to mirror, m	10
Pulse duration, s	2(equivalent)
Repetition rate	1 pulse per 20min.
Max. consumed power, MW	40(20)
Averaged power, kW	70(35)

Mirror coils

Table 1.2

Magnetic field on axis,T	13
Pulse duration, ms	150
Max. current, kA	20
Max. applied voltage, kV	6
Stored energy, MJ	1.65(in each coil)
Cross-section of conductor, mm x mm	2 x 70
Number of turns	180

I MAIN MAGNETS

As is well known, plasma confined in an axisymmetric magnetic field can be subjected to the flute-type instability[1]. To avoid tremendous plasma losses accompanying the instability development, pressure-weighted curvature of the field lines should be favorable for stability. In the GDT, this requirement can be met due to contributions from the regions beyond the mirrors where the plasma of sufficiently high pressure is flowing along favorably curved field lines [2,3]. We have started the design by optimizing the magnetic field lines to achieve MHD stable confinement. In the simulations we have used the mathematical model of a two-component plasma in the GDT[4]. This model calculates distribution functions of the sloshing ions using the Fokker-Plank equation and plasma parameters inside the expanders. The problem for sloshing ions is solved by making use of a semi-analytical approach developed in [4]. Spatial variation of parameters was taken into account by appropriate averaging of the coefficients over the plasma volume. By using this model we have optimized the geometry of the field lines near the turning points of the sloshing ions to reduce their unfavorable contribution to stability. The plasma inside the expander was simulated using adiabatic and isothermal approximations which can be applied at different electron temperatures. The model also takes into account limitations on maximum β -value, the validity of the paraxial limit in current points on a line, the ratio between local curvature radius and ion Larmor radius, etc.

Near the midplane, where the neutral beams are trapped, the magnetic field should be closely homogeneous to avoid enhanced initial spread of the sloshing ions over the

pitch angles. Given these limitations we have recalculated about 10 different versions of the magnetic system. Its final version is shown in Fig.2a. Design parameters of the coils are given in Table 1.3 which includes only half of them because the set is symmetric with respect to the trap center. Here z is a distance from midplane to coil center; r is an inner radius of the coil; $\Delta z \times \Delta r$ is the coil cross-section, n-number of sections per coil; N is the number of turns; NI is the total current in coil, kA. All dimensions are given in centimeters. The 7th coil consists of 8 sections which were previously used as a part of the magnetic system of the PSP-2 facility [5]. They are made of copper conductors of 25mm x 50 mm in cross-section with a hole of 15mm in diameter and 42mm x 50mm cross-section with a 20mm hole. These coils generate magnetic fields with high axial symmetry almost all over their inner diameters because of a special design of transition windings between the layers[5]. As it was already mentioned , these transitions may give dipole perturbations when a finite thickness of conductors is taken into account. Coil 8 is of the same design.

By now the production of the coils has been started in the INP machine shop. All of them (except coil 9 whose design is given in the next section) consist of sections of the same design and their manufacturing technology differs only due to difference in diameters and numbers of turns. Thus the magnetic system (excepting 7 and 9 coils) consists of only 5 standardized sizes of the sections which are used for assembling the coils. The largest coils 1 with an outer diameter of 3.7m consist of 5 sections and each of them is mounted on fixed supports. The other coils are installed on movable carts and are aligned with respect to the first one. The axial position of coils is determined by the spacers/stretchings which support the corresponding component of the ponderomotive forces.

All the coils (except coils 9 having separate power supplies) are connected in series. The coils 1 and 7 are incorporated into the common circuit being preliminary connected in parallel by pairs, so that their windings are carrying half the total current. Two rectifying units each of nominal power 20MW (voltage - 800V, nominal current - 25kA) are to be used to energize the magnets. One of them in future will be available and up to now it is used at the PSP-2 facility. During the single pulse the coils 1 and 7 are heated by 1.4 C and the remaining coils except for 9 - by 5.7 C. The mean power consumed by the coils is 67kW. We planned to remove the heat by distilled water using available heat-exchanger of 1 MW power. This heat-exchanger has enough capacity to keep the temperature of the coils close to required values. We also planned to switch on the cooling system during the baking of the vacuum chamber for outgassing. In this

regime it is used to prevent the overheating of the coils' insulation.

A section of a coil (Fig.2.c) consists of two flat spirals wound with the copper conductor of 25mm x 50mm in cross-section with a hole of 15 mm in diameter. The insulation between the turns and layers is made of fiberglass laminate impregnated with epoxy. The standard section with insulation is 103mm thick. The conductor's ends are connected with the end plates which have holes for connection with the water pipes.

The technological line has been developed and manufactured in the machine shop for manufacturing the coil sections. The main components of the line are the specially developed low-turn (with a large torsional moment) machine, a tightening device, a device for airtight soldering of the conductors, a milling machine for preparing the conductor's ends for soldering. Before the winding of the coils, the conductors pass through the line of preliminary preparation which has been also developed and manufactured at the machine shop. In this line the conductors are trimmed at both ends, undergo RF annealing and removal of scale. The conductors are soldered by a high temperature silver solder in the device assuring high quality connections. Each connection undergoes hydraulic tests for air tightness just after the soldering and after winding of the whole section. The insulation between turns and layers is continuously inserted during the winding of the section. The impregnation of sections is made by an epoxy of hot hardening by the " Monolith" method in a special mould. This method assumes a preliminary pumping of the vacuum-tighten mould and then polymerization under 10atm pressure. The temperature necessary for the polymerization of the epoxy (120°C) is provided by the overheated water flowing along the duct in the conductors. After the impregnation the section is exposed to the mechanical treatment over the outer diameter and side-ends which are used as bases for further assembly.

Parameters of the coils. Table.1.3

Coil	z-pos.	r	Δz	Δr	n	N	NI
1	120.25	135.00	51.50	46.70	5	180	2250.00
2	188.00	48.00	20.60	5.10	2	8	200.00
3	225.00	48.00	10.30	23.40	1	18	450.00
4	257.00	48.00	10.30	23.40	1	18	450.00
5	300.00	48.00	20.60	23.40	2	36	900
6	343.00	48.00	30.90	23.40	3	54	1360.00
7	423.70	42.50	82.40	59.00	8	292	3650.00
8	498.00	24.50	61.80	41.60	6	192	4800.00
9	490.00	9.50	14.60	10.50	1	180	3600.00
10	810.00	80.00	10.30	7.60	1	6	-150.00

II MIRROR COILS

The magnetic field in the mirror is composed of the 7 T field provided by the main coils and the field of the small size mirror coil 9 (Fig2, Table 1.2) whose contribution is 13T. This small radius coil is turned on when the current in the main coils attains its maximum. The pulse duration is 150ms, maximum current is 20kA. Other parameters of the mirror coil are given in Tabl. 1.2. Each mirror coil is powered by a capacitor bank with the stored energy of 1.65MJ. Structurally, the mirror coil is combined with a part of vacuum chamber providing the mirror unit as shown in Fig.3. The unit is attached to the chamber through the flanges 1 at its ends. The coil is put on the vacuum chamber of the unit with the radial gap of 1.75cm so that the coil and the chamber are not mechanically connected and can be individually fixed. The axial component of ponderomotive forces acting on the coil is counterbalanced by the other coils through the glass-fiber laminate flanges 9 bolted to each other. Inside the vacuum chamber the directly heated niobium liner 2 is placed, whose shape is similar to that of the vacuum wall. The mirror coil is the most tense component of the magnetic system by both, the mechanical as well as by the

thermal loads. Its design is made similar to that previously developed for the coils of the SPIN, GOL-3, GDL devices at the Budker INP[6,7,8]. The coil itself consists of two sections 4 and 5 made of a cold-rolled conductor of 2 mm x 70mm in cross-section. The sections are connected by the common inner loop. The total number of turns in the coil is 180. The sections are isolated between each other by 1 mm thick fiber-glass spacer. The insulation between turns is two layers of cable paper 0.08 mm thick. From its outside each section is rimmed by a fiber-glass band 7. After winding the coil is impregnated by epoxy with the use of the same technology as the central cell coils. The conductor, from which the coil is made of, is sand blasted before winding to improve the adhesion of the epoxy.

The coil is air-cooled between the shots from its side surfaces. The cooling air at 6 atm pressure is supplied through two circular collectors 10 in flanges 9 and then passes 45 radial slits where the heat is removed from the coil surface. After passage through the slits the air enters the cylindrical gap between the inner side of the coil and shield 3. This air-cooled shield serves to prevent the overheating of the inner part of the coil when the vacuum chamber is baked for conditioning. The air flows out of the mirror unit through the output collector 11. The accepted cooling scheme uses air instead of the commonly used water as coolant. Thus one avoids the use of of metallic components near the current-carring conductors, thereby increasing the coil overall reliability. Calculations show that during the operation cycle the conductor temperature doesn't exceed 70°C. In the standard regime of operation (1 pulse per 20 min.) the temperature is estimated to be 53°C just before the shot with 17°C raise during the pulse. The maximal tangential tensions occuring in the coil's turns at the mirror ratio of 20 approach 32kg/mm^2. These tensions are near the limit for cold-rolled copper.

III VACUUM SYSTEM

The vacuum system was developed to achieve base pressure less than 10^{-8} Torr in the central cell of the device. This involves the necessity of periodically heating the chamber up to at least 150-200°C for wall conditioning as well as the use of metal seals. The vacuum chamber shown in Fig.1 consists of the central cell chamber of 15m^3 in volume and two end tanks 5 of 10m^3 each. The chambers are attached by the mirror units 2 equiped with the compensating bellows 7. If necessary, the chambers can be isolated from each other by the gate valves 8 of ZPT-250 type. The main chamber and neutral beam ducts are isolated by the valves with innner clearance diameters of 750mm (11).

The central cell chamber consists of the central section 3 of 2400mm in diameter

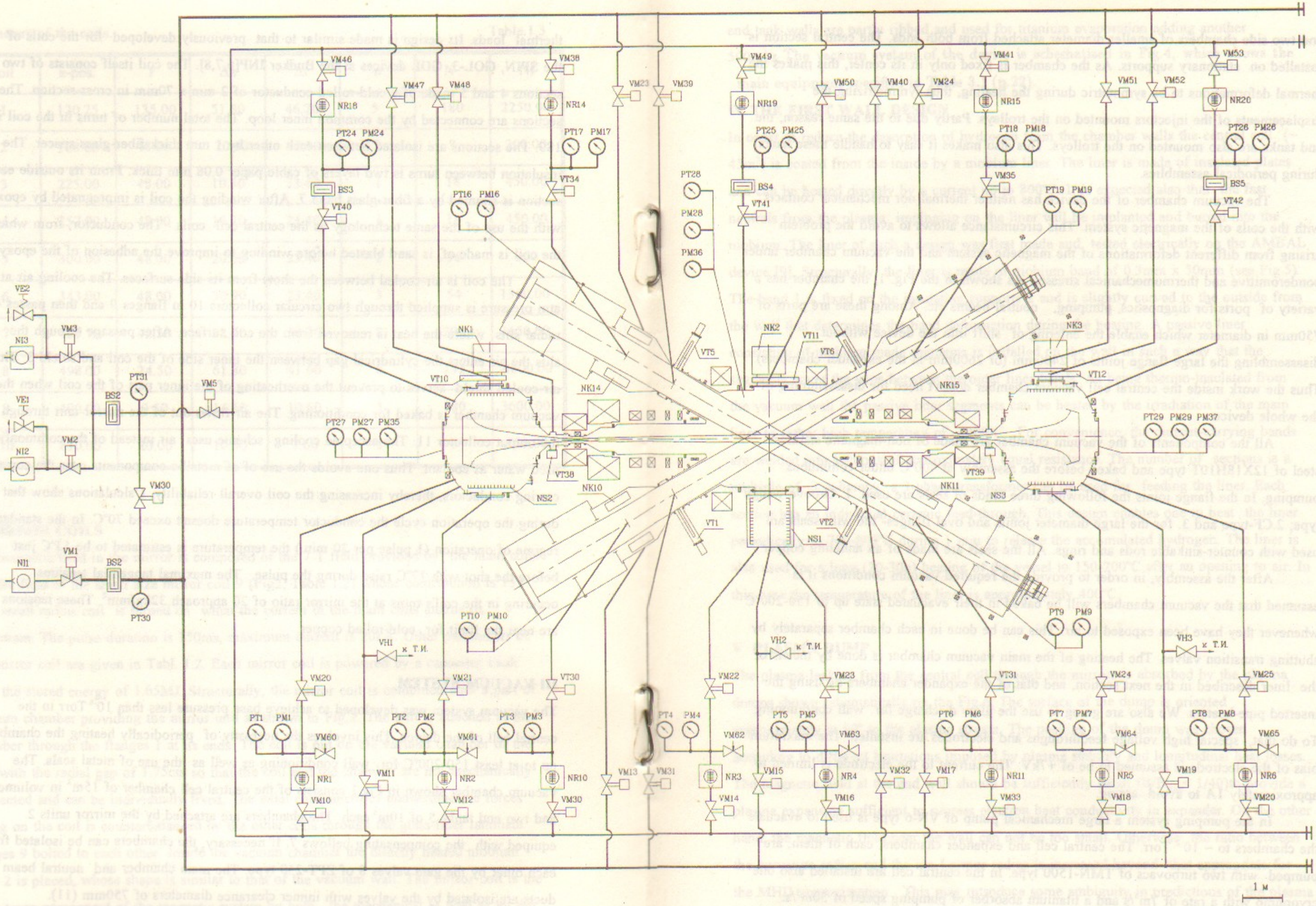

Fig.4 The HPNS vacuum system, specifications are given in Tabl.3.1 on p.22 .

and two side chambers of smaller diameter attached from both ends. The central section is installed on stationary supports. As the chamber is fixed only in its center, this makes the thermal deformations to be symmetric during the heating, thus symmetrizing the displacements of the injectors mounted on the trolleys. Partly due to the same reason, the end tanks are also mounted on the trolleys. This also makes it easy to handle these tanks during periodical assemblies.

The vacuum chamber of the device has neither thermal nor mechanical contacts with the coils of the magnetic system. This circumstance allows to avoid the problem arising from different deformations of the magnetic system and the vacuum chamber under ponderomitive and thermomechanical stresses. As shown in the Fig. 1, the chamber has a variety of ports for diagnostics, pumping, neutral beams etc. Among these are ports of 750mm in diameter which enable the entering of stuff into the device without disassembling the large flange joints of 2400mm (or 2600mm in the expander chambers). Thus the work inside the central cell vacuum chamber doesn't need for disassembling of the whole device.

All the components of the vacuum chamber are made of non-magnetic stainless steel of 12X18H10T type and baked before the assembly at 400°C under continuous pumping. In the flange joints the following three kinds of seals are used: 1. Groove-wedge type; 2.CF-type and 3. for the large diameter joints and oval flanges- the wire seals are used with counter-sinkable rods and rings. All the seals are made of an anneling copper.

After the assembly, in order to provide the required vacuum conditions it is assumed that the vacuum chambers will be baked in their evacuated state up to 150-200°C whenever they have been exposed to air. This can be done in each chamber separately by shutting transition valves. The heating of the main vacuum chamber is done by means of the liner described in the next section, and that of the expander chambers by using the inserted pipe-heaters. We also are going to use the glow discharge for wall conditioning. To do that, special high voltage feedthroughs and electrodes are installed. The maximum bias of the electrode is assumed to be of +7kV. The current to the electrode is limited to approximately 1A to avoid arcing.

In the pumping system a large mechanical pump of VN-6 type is used to evacuate the chambers to ~ 10^{-2} Torr. The central cell and expander chambers, each of them, are pumped with two turbovacs of TMN-1500 type. In the central cell are installed also one cryopump with a rate of $7m^3/s$ and a titanium absorber of pumping speed of $50m^3/s$. Additionally, the injectors are equipped with pumps with a total speed of $640m^3/s$. The

end tank walls are partly ribbed and used for titanium evaporation adding another $500m^3/s$. The vacuum system of the device is schematized in Fig.4, which shows the main equipment specified in Table 3.1 (p.22).

IV THE FIRST WALL DESIGN

In order to reduce the desorption of hydrogen from the chamber walls the central cell (~ $45m^2$) is coated from the inside by a niobium liner. The liner is made of insulated plates and can be heated directly by a current up to 800°C. It is expected also that the fast neutrals from the plasma impinging on the liner will be implanted and buried into the niobium. The liner of such a design was first made and tested electrically on the AMBAL device [9]. Structurally, the liner is made of niobium band of 0.3mm x 50mm (see Fig.5). The band 1 is fixed on the insulating supports 2 and is slightly curved to the outside from the wall that determines the band deformation during the heating. A passive liner consisting of niobium made segments is installed on the wall in such a way that the segments cover the gaps between the outer liner bands. As being thermo-insulated from the vacuum wall the passive liner segments can be heated by the irradiation of the main liner to rather high temperature of ~ 200°C . For convenience, the current-carrying bands are welded into sections of approximately equal resistance. The number of sections is a multiple of 3, whereby a 3-phase transformer can be used for feeding the liner. Each section has an individual ceramic feed-through. This design enables one to heat the liner periodically to 700-800°C during 1 min to release the accumulated hydrogen. The liner is also used for a long (20-30h) heating of the vessel to 150-200°C after an opening to air. In this case the temperature of the liner is approximately 400°C.

V PLASMA DUMP

The plasma leaking from the central cell through the mirrors is absorbed by the plasma dumps shown schematically on the Fig.6. The surface of the dump is oriented approximately at 90° to the plasma stream. The position of the dump was chosen according to different limitations imposed by plasma stability and longitudinal heat losses. The magnetic field at the end wall should be sufficiently small ($B/B_{max} < 1/40$)to provide a plasma expansion sufficient to supress electron heat conductivity in expander. On the other hand, the magnetic field near the wall can not be too small. Otherwise the ratio between the curvature radius and the ion Larmor radius is increased beyond that appropriate for the MHD approximation. This may introduce some ambiguity in predictions of the plasma stability. In certain cases the limitation on the maximum admissible ratio between the

plasma radius and the Larmor radius ρ_i of escaping ions becomes important. We have used the limitation on the curvature radius $\kappa\rho_i < 0.3$,where κ is a normal curvature, that is consistent with the value measured in the GDT experiment [10].

The plasma dump consists of a few separate end plates. Each of them serve to receive the plasma escaping from different radial regions of the entire volume. This allows to meet both diagnostic and control needs. As it is seen from Fig.6 the plasma occupying the region mapped on to the midplane to radii less than 1cm hits a disk-shaped plate 1 and a cylindrical plate 2. Plasma from larger radii flows on to the conical plate 3 that is made of four conical rings, each of them divided into 8 azimuthal segments. All the end plates are mounted on the insulating ceramic supports. Thus all of them can be electrically biased or grounded. The current flowing to each end plate can be measured separately. The end plates are made of stainless steel of 12X18H10T type. If needed the plates can be periodically heated by 25 quartz halogen lamps 5 up to 400°C for degassing. For heating of the plates the halogen lamps of KG 220-2000-2 type are fixed on their back sides. To increase their reliability and lifetime they are supplied with half of the nominal power, totalling 25kW. We expect that in a long pulse regime of operation enhanced pumping speed will be required to sustain the gas pressure near the wall less than 10^{-3}Torr. For that case the surface of the end plates can be covered with a titanium film by using arc-evaporators 6. Simultaneosly , the inner surface of the expander end tank is also covered by titanium. In order to increase the pumping speed this surface is ribbed (7). Shield 8 is envisaged to protect the quartz lamps against the evaporation as well as the electrical equipment located behind the end plates.

The geometry of the field lines shown on the Fig.6 has been optimized to obtain the maximum possible contribution of the expanders to pressure-weighted curvature under restrictions discussed at the beginning of this section. Simultaneously we have adjusted the profile of the magnetic field in the central cell to minimize its unfavorable contribution to stability. We have evaluated plasma stability in the magnetic field generated by the magnets using the criterion for the localized MHD-modes [2,3]. According to these considerations, the HPNS plasma parameters are predicted to be sufficiently well within the stable region.

ACKNOWLEGMENTS

The authors wish to thank Dr. H. Kumpf (FZ Rossendorf, Germany) for his support and interest throughout this work. Helpful discussions with Prof. V.I.Volosov (Budker INP) contributed a lot to improvements of the design and are also highly appreciated. This work has been supported in part by the Federal Ministry of Science and Technology of the Federal Republic of Germany through a research contract code FZR 199333 mediated by FZ Rossendorf.

REFERENCES

1. Nagornyj V.P., Ryutov D.D., Stupakov G.V., Nuclear Fusion,v.24, 11(1984)1421.

2. Mirnov V.V., Ryutov D.D., *Voprosy Atomnoj Nauki i Tekhniki – Termoyadernyj Sintez* , v.1 (1980) 57 (in Russian).

3. MirnovV.V., Nagornyj V.P., Ryutov D.D. , *Preprint INP 84-40* (Institute of Nuclear Physics, Novosibirsk, 1984) (in Russian).

4. Kotel'nikov I.A., Ryutov D.D., Tsidulko Yu.A., Kat'ishev V.V., Komin A.V., Krivosheev V.M., *Preprint INP 90-105* (Institute of Nuclear Physics, Novosibirsk, 1990) (in Russian).

5. Abdrashitov G.F., Volosov V.I., Schreiner K.K., *Voprosy Atomnoj Nauki i Tekhniki – Termoyadernyj Sintez* , v.1 (1981) 19 (in Russian).

6. Davydenko V.I., Ivanov A.A.,*et al., Preprint INP 86-104* (Institute of Nuclear Physics, Novosibirsk, 1986) (in Russian).

7. Persov M.V., Livshits A.A., Schreiner K.K., Khrestolyubov V.S., Kuznetsov G.F., IEEE Trans. on Magnetics, v.28, 1(1992)255.

8. Voropaev S.G., Gorbovsky A.I., Knyazev B.A., Lebedev S.V., Nikolaev V.S., Sheglov M.A., *Preprint INP 85-107* (Institute of Nuclear Physics, Novosibirsk, 1985) (in Russian).

9. Dimov G.I., *Preprint INP 87-150* (Institute of Nuclear Physics, Novosibirsk, 1987) (in Russian).

10. Anikeev A.V., Bagryansky P.A.,*et al., Proc. of Int. Conf. on Open Systems for Mag. Fusion*, Novosibirsk, 1992. (to be published)

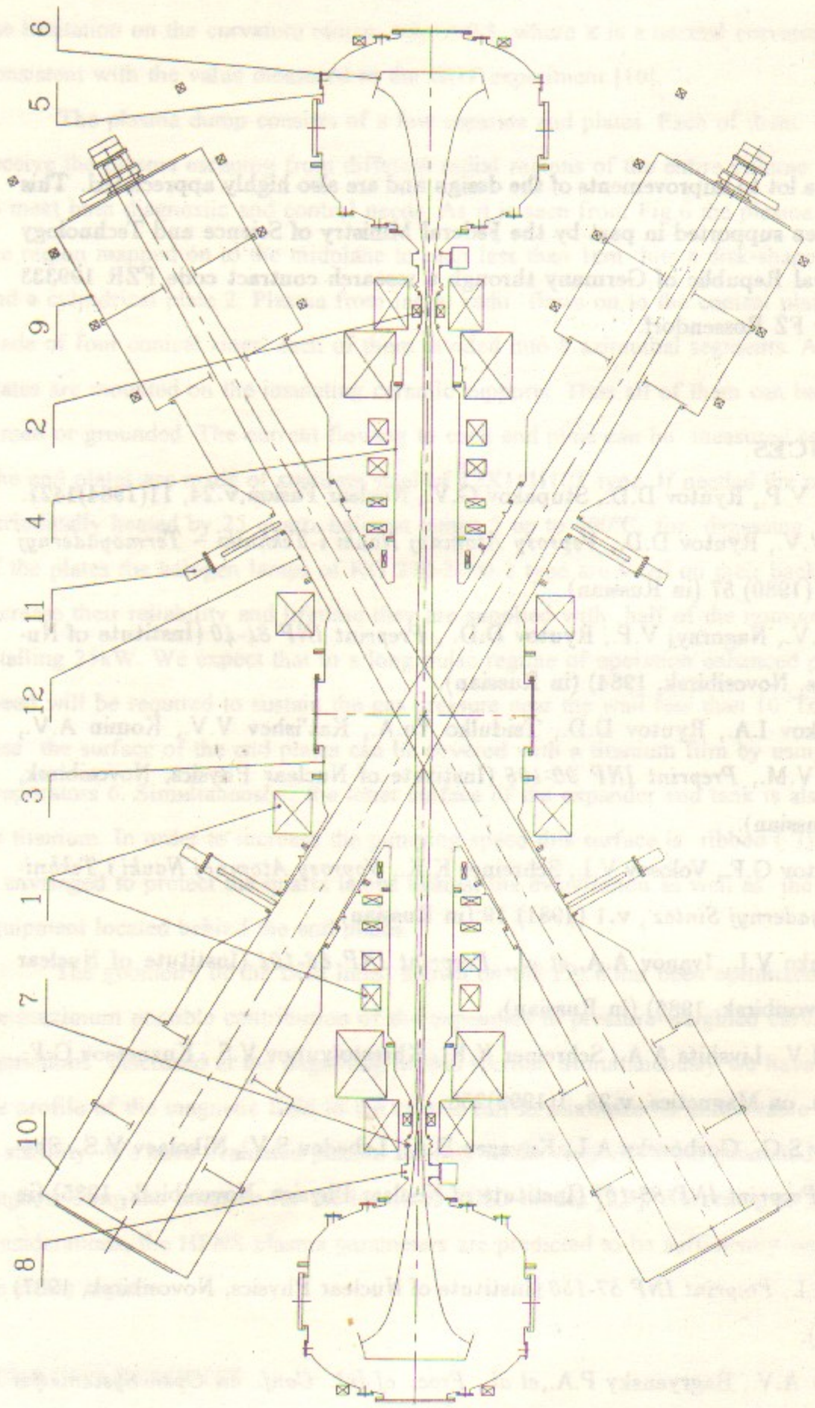

Fig.1. Layuot of the HP facility: 1-central cell coils, 2-choke coil, 3-central vacuum chamber, 4-side section, 5-expander, 6-plasma dump, 7,12-bellows, 8,11-gate valve, 9-neutral beam injector, 10-beam dump

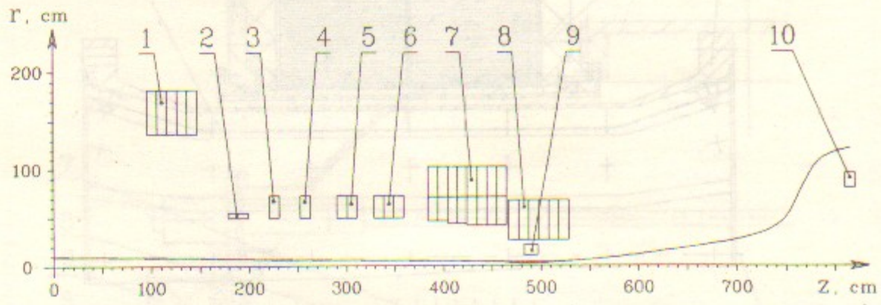

a

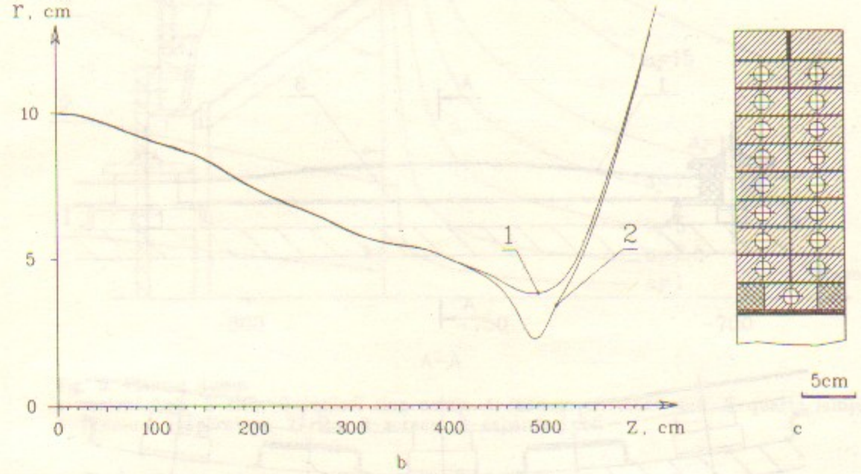

Fig.2. a-HPNS magnets, parameters of the coils are given in Tabl. 1.1-1.3 ; b-magnetic field lines: 1-coil 9 on, 2-coil 9 off ; c-cross-section of a coil.

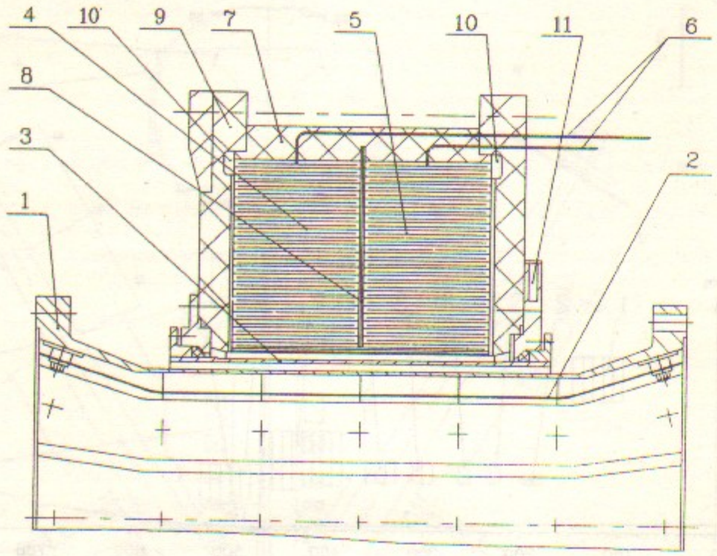

Fig.3. Layout of mirror magnet.
1–vacuum chamber wall; 2–Nb–liner; 3–screen; 4,5–winding of coil; 6–feeds; 7–spacer; 8–insulating disk (glass cloth laminate); 9–side flanges; 10,11–air feeders.

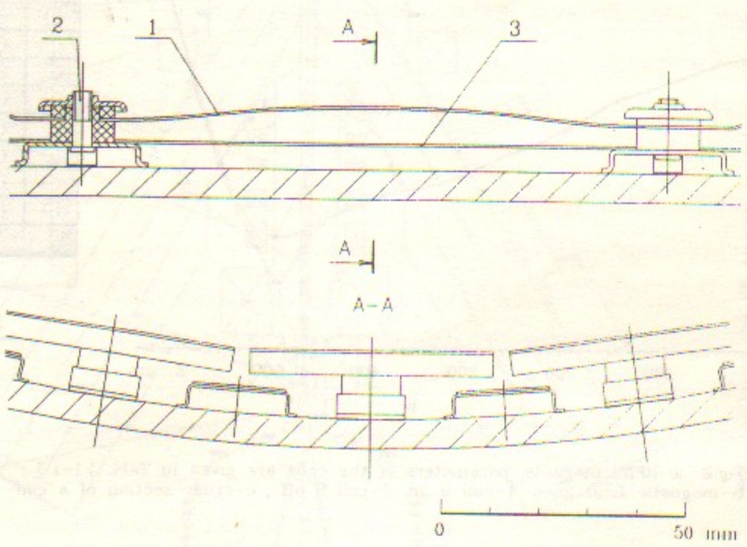

Fig. 5. Nb–liner.
1 current–carring bend, 2 ceramic holder, 3–passive liner.

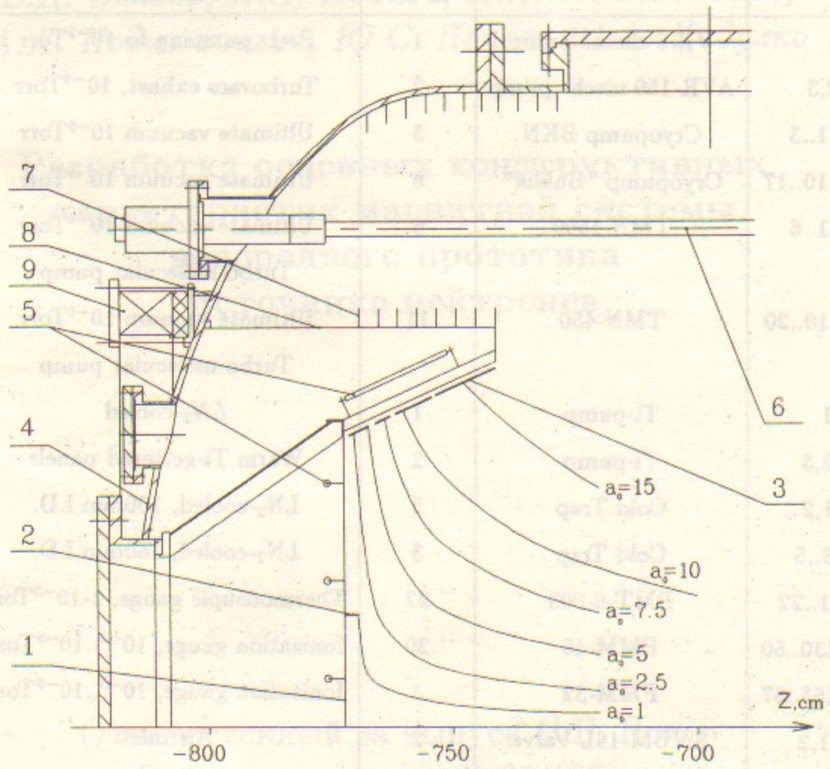

Fig. 6. Plasma dump.
1–central disk; 2–riny; 3–conical ring array; 4–vacuum chamber wall; 5–quartz lamps; 6–titanium evaporators; 7–ribs; 8–screen; 9–expander coil.

Specifications of the vacuum equipment. Table 3.1

	Type of equipmemt	Number in use	Parameters Functions
NI1	VN-6 mech. pump	1	Prel. pumping to 10^{-2}Torr
NI2,3	AVR-150 mech. pump	2	Turbovacs exhast, 10^{-3}Torr
NK1..3	Cryopump BKN	3	Ultimate vacuum 10^{-6}Torr
NK10..17	Cryopump "Bublik"	8	Ultimate vacuum 10^{-6}Torr
NR1..6	TMN-1500	6	Ultimate vacuum 10^{-9}Torr Turbo-molecular pump
NR10..20	TMN-450	11	Ultimate vacuum 10^{-9}Torr Turbo-molecular pump
NS1	Ti-pump	1	LN_2-cooled
NS2,3	Ti-pump	2	Warm Ti-gettered panels
BS1,2	Cold Trap	2	LN_2-cooled, 100mm I.D.
BS3..5	Cold Trap	3	LN_2-cooled, 160mm I.D.
PT1..22	PMT-6-003	22	Thermocouple gauge, $1\text{-}10^{-3}$Torr
PM30..50	PMM-46	20	Ionization gauge, $10^{-3}..10^{-9}$Torr
PM55..57	PMM-32	3	Ionization gauge, $10^{-3}..10^{-9}$Torr
VE1,2	KVUM-16L Valve	2	Air inlet
VH1..3	25mm I.D. Valve	3	
VM1..4	2EVE-100 Valve	4	
VM10..26	VEP-63 Valve	17	
VM30..53	VEP-25 Valve	24	
VM60..65	NET	6	Controlable leak
VT1..8	Gate valve	8	750mm I.D.
VT10..12	Gate valve	3	630mm I.D.
VT20..25	ZPT-250	6	Bakeable valve
VT30..42	ZPT-160	13	Bakeable valve

А.С. Александров, А.И. Горбовский, В.В. Мишагин,
А.В. Ситников, К.К. Шрайнер, Г.Ф. Абдрашитов,
Е.Д. Бендер, А.А. Иванов, И.А. Котельников,
А.А. Подыминогин, Ю.С. Попов, Ю.А. Цидулко

Разработка основных конструктивных характеристик магнитной системы водородного прототипа источника нейтронов

Ответственный за выпуск С.Г. Попов
Работа поступила 31.01 1994 г.

Сдано в набор 5 января 1994 г.
Подписано в печать 1 февраля 1994 г.
Формат бумаги 60×90 1/16 Объем 1.7 печ.л., 1.4 уч.-изд.л.
Тираж 250 экз. Бесплатно. Заказ N° 7

Обработано на IBM PC и отпечатано на
ротапринте ИЯФ им. Г.И. Будкера СО РАН,
Новосибирск, 630090, пр. академика Лаврентьева, 11.